Protoplasma (2016) 253:1159–1174
DOI 10.1007/s00709-015-0876-4

ORIGINAL ARTICLE

An antifungal protein from *Ginkgo biloba* binds actin and can trigger cell death

Ningning Gao[1] · **Parvesh Wadhwani**[2] · **Philipp Mühlhäuser**[2] · **Qiong Liu**[1] · **Michael Riemann**[1] · **Anne S. Ulrich**[2,3] · **Peter Nick**[1]

Received: 1 June 2015 / Accepted: 17 August 2015 / Published online: 28 August 2015

Abstract Ginkbilobin is a short antifungal protein that had been purified and cloned from the seeds of the living fossil *Ginkgo biloba*. Homologues of this protein can be detected in all seed plants and the heterosporic fern *Selaginella* and are conserved with respect to domain structures, peptide motifs, and specific cysteine signatures. To get insight into the cellular functions of these conserved motifs, we expressed green fluorescent protein fusions of full-length and truncated ginkbilobin in tobacco BY-2 cells. We show that the signal peptide confers efficient secretion of ginkbilobin. When this signal peptide is either cleaved or masked, ginkbilobin binds and visualizes the actin cytoskeleton. This actin-binding activity of ginkbilobin is mediated by a specific subdomain just downstream of the signal peptide, and this subdomain can also coassemble with actin in vitro. Upon stable overexpression of this domain, we observe a specific delay in premitotic nuclear positioning indicative of a reduced dynamicity of actin. To elucidate the cellular response to the binding of this subdomain to actin, we use chemical engineering based on synthetic peptides comprising different parts of the actin-binding subdomain conjugated with the cell-penetrating peptide BP100 and with rhodamine B as a fluorescent reporter. Binding of this synthetic construct to actin efficiently induces programmed cell death. We discuss these findings in terms of a working model, where ginkbilobin can activate actin-dependent cell death.

Keywords Antifungal protein · Actin · Cell-penetrating peptide · Programmed cell death

Handling Editor: Jaideep Mathur

Electronic supplementary material The online version of this article (doi:10.1007/s00709-015-0876-4) contains supplementary material, which is available to authorized users.

✉ Peter Nick
peter.nick@kit.edu

[1] Molecular Cell Biology, Botanical Institute and DFG-Center of Functional Nanostructures (CFN), Karlsruhe Institute of Technology (KIT), Kaiserstr. 2, 76128 Karlsruhe, Germany

[2] Institute for Biological Interfaces (IBG-2), KIT, P.O. Box 3640, 76021 Karlsruhe, Germany

[3] Institute of Organic Chemistry and CFN, KIT, Fritz-Haber-Weg 6, 76131 Karlsruhe, Germany

Introduction

Plants as sessile organisms cannot run away when they are attacked nor can they rely on mobile defence cells that constitute the core of animal immunity. Instead, plant defence is based upon the innate immunity of individual cells. This innate immunity is composed of two layers (Jones and Dangl 2006): on the one side is a broad-spectrum basal defence, which can be triggered by microbial associated molecular patterns (MAMP) and activate the production of secondary metabolites or proteins with antimicrobial activity. Specialized pathogens have adapted to this host response by so-called effector molecules which can suppress this basal defence, such that the pathogen can invade the host cell. On the other side, during the coevolution with these pathogens, some host plants have acquired specific receptors that can recognize the microbial effectors and reactivate defence. As final response to microbial invasion, this effector-triggered immunity (ETI) can culminate in programmed cell death. Cell-death-related immunity is a very effective strategy to kill or at least to contain the intruder, but it is a meaningful strategy only in organisms where cells have developed a high degree of functional cooperation. Cell-death-related immunity is therefore not expected

in most of the algae where true multicellularity has not been fully achieved but must have evolved later during the evolution of terrestrial plants. Nonetheless, there is evidence for a second, possibly independent development of cell-death-related immunity in the kelps, macroalgae that have developed true multicellularity as well (for review see Weinberger 2007). The finding that programmed cell death has been discovered also in clonal unicellular microorganisms, for instance in yeasts, indicates that cell-death-related immunity might have evolved from biofilm-related precursors (Severin and Hyman 2002).

Secretion of toxic compounds is therefore considered to be the primary and most ancient tool of defence. In fact, there is a rich literature describing such compounds from lower plants including mosses (for review see Ponce de Leon and Montesano 2013), ferns (Banerjee and Sen 1980; Lin et al. 2000; Parihar et al. 2010), and algae (Kubanek et al. 2003). Production and secretion of these compounds are expected to be inducible for mainly two reasons: (a) It sequesters considerable metabolic activity, which is thus not available for normal growth and development and (b) these compounds are toxic, so one strategy to evade autointoxication of the producer cell or tissue is to strictly confine the production of these compounds to the time when they are needed and to the location where they are needed.

The invention of seeds as mobile and robust means for gene flow has confronted plant defence with a new challenge: as an adaptation to the propagation function, maturating seeds shut down metabolic activity almost completely. A structure that is densely packed with rich biological resources and at the same time is metabolically inactive represents a very attractive target for microbial attack. Since, under these circumstances, inducible defence does not provide an efficient strategy to ward off pathogens from seeds, seed plants (and possibly already the heterosporic ferns, such as *Selaginella*) must have evolved constitutive protection against fungal attack.

Ginkgo biloba as a 'living fossil' represents one of the most ancestral lines in the gymnosperms and therefore might serve as an interesting model to address the question about the evolution of seed immunity. In fact, *Ginkgo* seems to be highly resistant to pathogens, which may be the reason why this unique tree can live up to 2500 years. In fact, this species is rich in pharmacologically active compounds that are also exploited for medical applications including antioxidant, neurotransmitter/receptor modulatory, and anti-platelet activating activities (for review see Diamond et al. 2000). *Ginkgo* has been used not only as source of food (the roasted embryo sack) but also in traditional medicine. Under the traditional name *Bai Guo* it is used due to its vasodilating activity, for instance, to cure hypertension and dementia (Kleijnen and Knipschild 1992). A jasmonate-dependent defensin gene (Shen et al. 2005) and a chitin-binding antimicrobial protein (Huang et al. 2000) cloned and purified from *G. biloba* leaves provide further evidence for efficient inducible basal immunity in this species.

The general question of seed immunity is even accentuated in *G. biloba*, because the immature seed is shed several months before fertilization actually takes place, which means that the delicate gametophytes have to survive for a long period amidst of the progressively rotten fleshy tissue. In fact, seeds of *G. biloba* contain high levels of the antifungal protein ginkbilobin (Wang and Ng 2000) that exhibits sequence similarity to embryo-abundant proteins mainly from gymnosperms, and a homology with the extracellular domain of angiosperm cysteine-rich receptor-like kinases (Sawano et al. 2007; Liu et al. 2010). The angiosperm homologues of ginkbilobin share the characteristic feature of receptor-like kinases, such as the N-terminal signal peptide, an extracellular domain (which is the domain exhibiting the homology with ginkbilobin), a transmembrane region, and a C-terminal domain with eukaryotic kinase signatures (for review see van der Geer et al. 1994). Ginkbilobin has been purified in two versions–the full-length protein contains a signal peptide and is termed ginkbilobin-2, while the first discovered ginkbilobin-1 is a fragment lacking the signal peptide and the DUF26 domain harbouring a characteristic cysteine signature, which is conserved between all plant homologues of ginkbilobin including the angiosperm receptor-like kinases (Wang and Ng 2000; Sawano et al. 2007).

To get insight into the potential cellular targets of ginkbilobin, we expressed green fluorescent protein (GFP) fusions of full-length and various truncated ginkbilobin in tobacco BY-2 suspension cells. We show that the signal peptide confers efficient secretion of ginkbilobin. When this secretion is prevented by cleaving off or masking the signal peptide, ginkbilobin decorates filamentous structures. Via different covisualization strategies, it is shown that these structures are actin filaments and that the actin-binding activity of ginkbilobin is located in a specific subdomain (termed as A1), just downstream of the signal peptide. This subdomain can coassemble with actin in vitro, indicative of direct binding to actin. Upon stable overexpression of this domain, we observe a specific delay in premitotic nuclear positioning indicative of a reduced dynamicity of perinuclear actin cables. To gain insight into the cellular events evoked by the binding of this subdomain to actin, we employ a strategy based on chemical engineering using synthetic peptides. They comprise of different parts of the actin-binding subdomain conjugated with the cell-penetrating peptide BP100 and with rhodamine B (RhB) as a fluorescent reporter. We observe that the binding of specific subdomain motifs to actin filaments is followed by rapid and efficient induction of cell death, meeting the criteria of a programmed cell death response such as TdT-mediated dUTP-biotin nick end labeling (TUNEL) labelling and nuclear disintegration. This cell death can be quelled by pretreatments that prevent actin bundling, such as low concentrations of

latrunculin B or elevation of cellular auxin content. These observations lead to a working model, where ginkbilobin can interfere with actin remodelling, activating a pathway culminating in programmed cell death.

Materials and methods

Cell lines and cultivation

Suspension cell lines of BY-2 (*Nicotiana tabacum* L. cv bright yellow-2; Nagata et al. 1992) were cultivated in liquid medium containing 4.3 g l^{-1} Murashige and Skoog salts (Duchefa Biochemie, Haarlem, Netherlands), 30 g l^{-1} sucrose, 200 mg l^{-1} KH_2PO_4, 100 mg l^{-1} inositol, 1 mg l^{-1} thiamine, and 0.2 mg l^{-1} 2,4-D, pH 5.8. The cells were subcultivated weekly by inoculating 1–1.5 ml of stationary cells into 30 ml fresh medium in 100 ml Erlenmeyer flasks. The cells were incubated at 27 °C in the dark on an orbital shaker (IKA Labortechnik, Staufen, Germany) at 150 rpm. Other than the BY-2 wild type (WT) (Nagata et al. 1992), two transgenic cell lines, GF11 (Sano et al. 2005) and FABD2 (Klotz and Nick 2012), were used in this study which express the actin-binding domain 2 of plant fimbrin in fusion with GFP and RFP respectively under the control of the constitutive CaMV 35S promoter. In addition, several stable transgenic cell lines were generated in this work expressing different domains of ginkbilobin in fusion with GFP. Transgenic cell lines were cultivated in the same medium as BY-2 WT cell cultures, supplied with the respective antibiotics (100 mg l^{-1} kanamycin for the ginkbilobin cell lines and BY-FABD2-RFP, 30 mg l^{-1} hygromycin for GF11, respectively).

Cloning of full-length and truncated versions of ginkbilobin-2

Mature seeds of *G. biloba* were collected in Freiburg (Germany) in December and kept at −80 °C. The material was ground in liquid nitrogen using a mortar, and the total RNA was extracted following the improved RNA extraction method by Liu et al. (2010). cDNA synthesis was performed using the Dynamo cDNA Synthesis Kit (Finnzymes, Vantaa, Finland) according to the instruction of the manufacturer, taking 1 μg of RNA as template for reverse transcription. To generate transgenic cell lines overexpressing full-length or truncated versions of ginkbilobin-2, binary vectors were constructed using the Gateway® Cloning technology (Invitrogen Corporation, Paisley, UK). The gateway primers were designed according to the protocol of the manufacturer's instruction amplifying either full length, signal peptide, full length without signal peptide (NSP or ΔSP), subdomain A1, A1+A2, A1+A2+A3, and B of ginkbilobin-2 from the cDNA of *G. biloba*. The primer sequences are specified in supplemental Table 1. For the preparatory PCR, standard conditions and the Phusion polymerase (0.4 U for a total volume of 20 μl) were used with 35 cycles (pre-heating at 98 °C for 30 s; denaturation at 98 °C for 10 s, annealing at 58 °C for 20 s, and extension at 72 °C for 20 s), followed by final extension at 72 °C for 5 min. The size of the PCR products was verified by electrophoresis and purified using the NucleoSpin® Extract II (Macherey-Nagel, Dueren, Germany) kit according to the manufacturer's instruction. The resulting coding sequences were inserted into the binary vector pK7FWG2,0 (Karimi et al. 2002) or pK7WGF2,0 (Karimi et al. 2002) following the manufacturer's instruction. The structure of the different domains is shown in Fig. 1b.

Biolistic transformation

For biolistic transformation, gold particles (1.5–3.0 μM; Sigma-Aldrich, Germany) were coated with 1 μg of plasmid DNA modified from a manual of Bio-Rad (PDS-1000/He Particle Delivery System Manual). The coated gold particles were loaded on macrocarriers (Bio-Rad Hercules, CA, USA). Amount of 750 μl of 3-day-old BY-2 WT cells was placed on PetriSlides™ (Millipore, Billerica, USA) containing solid MS medium (0.8 %*w*/*v* Danish agar). These loaded PetriSlides™ were transferred into a custom-made chamber (Finer et al. 1992) and bombarded by three shots at a pressure of 1.5 bar in a vacuum chamber of −0.8 bar. After the bombardment, the cells were incubated for 18–48 h in the dark at 27 °C and then inspected by microscopy. For the cotransformation of two constructs, 500 ng of each plasmid was mixed before coating the gold particles.

Agrobacterium-mediated transformation

BY-2 cells were transformed via agrobacteria-mediated transformation following the protocol developed by Buschmann et al. (2011) with a few modifications for both transient or stable transformation. Chemo-competent *Agrobacterium tumefaciens* (LBA4404; Invitrogen Corporation, Paisley, UK) cells were used for the transformation. First, the cocultivation temperature was decreased to 22 °C instead of 27 °C which produced higher transient transformation rate. Second, the mixture of cells and agrobacteria was not directly placed on the MS Paul agar surface but on a layer of filter paper in between instead to avoid the mechanical wounding caused by transferring the cells when using a sterile spatula. For cotransformation, the cocultivation inoculum was prepared as mixture of the respective transformed *Agrobacterium* strains.

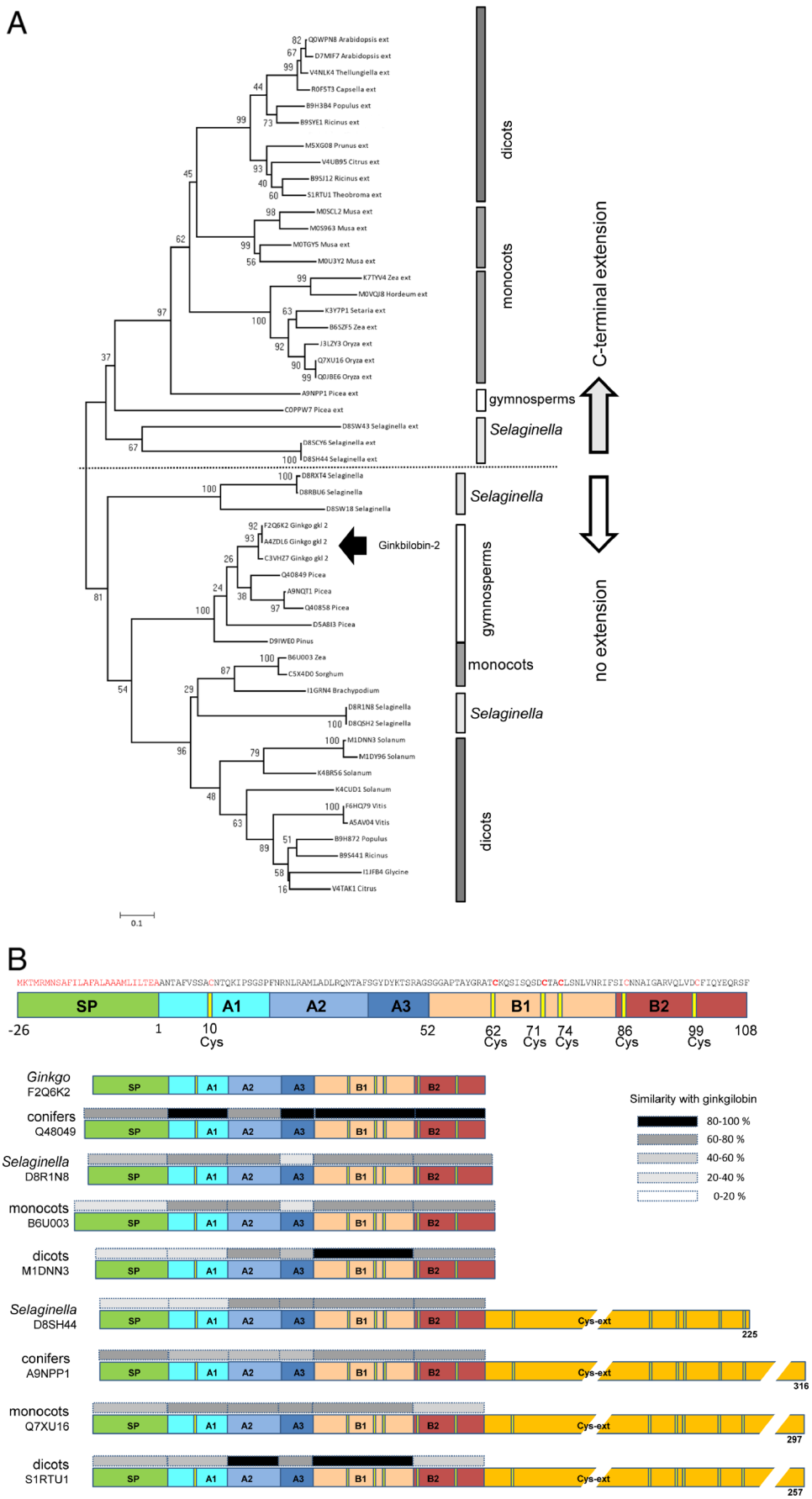

Fig. 1 Phylogeny and domain structure of ginkbilobin-2 related proteins. **a** Evolutionary relationship between 55 ginkbilobin-2 related protein sequences inferred by neighbour-joining method based on an alignment constructed by the ClustalW algorithm (see supplemental material 1). Values next to the branches represent the percentage of replicate trees in which the associated taxa clustered together in the bootstrap test (based on 500 replicates). The tree is drawn to scale, with branch lengths in the same units as those of the evolutionary distances used to infer the phylogenetic tree. The evolutionary distances were computed using the Poisson correction method and are in the units of the number of amino acid substitutions per site. All positions containing gaps and missing data were eliminated from the dataset (complete deletion option), leaving a total of 89 positions in the final dataset. The Swissprot accessions are given along with the genus name. **b** Domain structure of ginkbilobin-2 related protein sequences. SP-predicted signal peptide, followed by subdomains A1–A3 and subdomains B1, B2, and in some of the proteins an additional long cysteine-rich C-terminal extension (*Cys-ext*). The conservation of the individual domains with ginkbilobin-2 is indicated by the *shaded boxes* based on similarity at the amino acid level. The *yellow lines* represent conserved cysteine signatures

Treatment with actin drugs and phalloidin-based actin staining

To eliminate actin filaments, 1 μM of latrunculin B (Sigma-Aldrich, Deisenhofen, Germany) was added to the 3-day-old BY-2 cells (overexpressors of ginkbilobin subdomain A1, NSP/ΔSP, and actin marker line GF11), and the response was followed under the microscope. To visualize actin, the modified tetramethylrhodamine B isothiocyanate (TRITC)-phalloidin staining method by Maisch et al. (2009) based on the protocol by Olyslaegers and Verbelen (1998) was used. The cells were directly viewed under the microscope following three times washing for 10 min in phosphate-buffered saline.

Phenotyping cellular responses

The different ginkbilobin-2 based overexpressor lines were phenotyped as described in Kühn et al. (2013). Nuclear positioning was quantified from 1500 individual cells collected from three independent experimental series. The mitotic index (MI) was measured as described in Maisch and Nick (2007). The fluorescent dye Hoechst 22358 (Sigma-Aldrich, Neu-Ulm, Germany) intercalating into the DNA was used to discriminate non-mitotic from mitotic cells. Each data point was scored from a sample of 3000 individual cells from three independent experiments. Mortality in response to ginkbilobin-2 subdomain peptide conjugates was quantified by Evans Blue as described in Kühn et al. (2013). Each data point represents 3000 cells from three independent experimental series. To check whether the cells that die show features of programmed cell death, cells were fixed in Carnoy fixative [3:1 (*v*/*v*) 96 % (*v*/*v*) ethanol/acetic acid] complemented by 0.5 % (*w*/*v*) Triton X-100, and nuclei were labelled by TUNEL (in situ cell death detection kit, TMR red, Roche Diagnostics, Heidelberg Germany) following the protocol of the producer. DNA was counterstained by 1 μg/ml 2′-(4-hydroxyphenyl)-5-(4-methyl-1-piperazinyl)-2,5′-bi-(benzimidazole)-trihydrochloride (Hoechst 33258; Sigma, Taufkirchen, Germany). The antifungal activity of the peptides was tested against *Candida albicans* using previously described method (Wiegand et al. 2008). The antimicrobial activity of the conjugates against *C. albicans* was determined from dose-response series as described in Tsai et al. (2011).

Synthesis of ginkbilobin subdomain peptide conjugates

The subdomains A1, A2, and A3 from the putative actin-binding domain of ginkbilobin-2 were synthetically generated as fusions with the cell-penetrating peptide BP100 and rhodamine B, following the strategy previously described in Eggenberger et al. (2011). All peptides were synthesized using standard 9-fluorenylmethoxycarbonyl (Fmoc) solid-phase peptide synthesis (Fields and Noble 1990). Rhodamine B (RhB) was used as a fluorescent marker and BP100 as the cell-penetrating carrier. Rhodamine B was coupled at the N terminus of BP100, and the different ginkbilobin-2 subdomain peptides were coupled at the C termini of the constructs. The sequences of the peptide conjugates are specified in supplemental Table 2. The peptides were purified by HPLC using acetonitrile/water gradients as previously described (Wadhwani et al. 2006; Wadhwani et al. 2008), and the purified peptides were characterized by analytical liquid chromatography combined with ESI-mass spectrometry (Eggenberger et al. 2011).

Actin-binding assays

Actin filaments were polymerized from monomeric rabbit skeletal muscle actin purchased from Cytoskeleton (Denver, USA) according to the manufacturer's instruction. For the characterization of the binding behaviour of domain A1 conjugate to microfilaments, cosedimentation assays were performed according to Srivastava and Barber (2008). Amount of 50–100 μM of domain A1 conjugate was incubated with 25 μM G-actin in a 50 μl reaction volume in actin-binding buffer (10 mM Tris-HCl pH 7.0, 1 mM EGTA, 0.1 mM $CaCl_2$, 2 mM $MgCl_2$, 0.5 mM DTT, 1 mM ATP) for 1 h at 22 °C. The samples were centrifuged at 185,000 g for 20 min at 22 °C in a TLA-100 ultracentrifuge (Beckman, Krefeld, Germany) to sediment the filaments and the filament-bound protein. Equal amounts of the sediment and supernatant samples were separated by 15 % (*w*/*v*) SDS-PAGE and stained with Coomassie Brilliant Blue.

Microscopy

To phenotype cellular responses, cells were observed and recorded under an AxioImager Z.1 microscope (Zeiss, Jena, Germany). Images were analysed using the AxioVision (Rel. 4.8.2) software or Image J (NIH, Bethesda, USA). To observe the cellular details of the transformed cells, images of RFP-/TRITC and GFP-/Alexa Fluor® 488 fluorescence were acquired through an Axio Observer Z1 (Zeiss, Jena, Germany) using a 63 × /1.44 DIC oil objective , the 561 nm and 488 nm emission lines of the Ar-Kr laser, and a spinning-disc device (YOKOGAWA CSU-X1 5000). The apparent thickness of actin cables in response to ginkbilobin was quantified as described in Chang et al. (2015).

Results

Divergent phylogeny of proteins containing a ginkbilobin-2 domain

To access the putative functions of ginkbilobin-2, a phylogenetic tree was constructed based on the neighbour-joining

algorithm of homologous proteins (Fig. 1a). Homologues of ginkbilobin-2 could be identified only in seed plants, and in the heterosporic fern *Selaginella*. These homologues are clustered into two classes (Fig. 1b)–one class contained proteins just composed of the ginkbilobin-2 domain along with an N-terminal putative signal peptide for secretion, while the other class contained proteins harbouring, in addition, a long C-terminal extension of usually ~180 amino acids. Both classes occurred in all taxa, but there was a clear dominance of the version without extension in the gymnosperms, whereas the version with extension dominated in the angiosperms. For several angiosperm taxa, several homologues were found. Some of them are not significantly different (as shown exemplarily for soybean), whereas some are significantly different and fall into different subclades (as shown exemplarily for banana). In *Selaginella*, eight ginkbilobin-2 homologues could be identified: three with and five without this C-terminal extension. Within each of the two classes of ginkbilobin-2 domain proteins, the members clustered mostly in accordance with taxonomic relationship, i.e. dicot and monocot, as well as the gymnosperm members formed separate subclades. However, those homologues from *Selaginella* that lacked the C-terminal extension were split into two groups, one was basal to the clade, whereas the other clustered with the monocots, however, with a low bootstrap value. Alignment of the sequences revealed specific cysteine signatures that were conserved throughout, even between the accessions with and without the C-terminal extension. In this extension, further cysteine signatures could be detected that were preserved as well (Fig. 1b). The closest relatives of ginkbilobin-2 with approximately 85 % identity were embryo-abundant proteins from conifers. In *Ginkgo*, a closely matching second protein, designated as ginkbilobin-1, had been described as well (Wang and Ng 2000). However, since this protein was lacking a signal peptide and even a start codon, we considered this as a fragment and did not analyse it further. Based on the conservation in the alignment, the ginkbilobin-2 domain could be subdivided into subdomains A1, A2, A3, B1, and B2. Among those subdomains, especially B1 and A2 were conserved throughout the evolution of vascular plants, whereas A3 appeared to be more variable. The domain B contained a conserved cysteine signature C-X_8-C-X_2-C, which is a characteristic feature of a receptor superfamily described for *Arabidopsis thaliana* and rice and was proposed to participate in defence signalling (Chen 2001). However, these receptors do not share a ginkbilobin-2 domain.

The conservation of the cysteine signatures along with numerous other motifs of the ginkbilobin-2 domain throughout the evolution of vascular plants suggests that these motifs confer important biological functions. Since the ginkbilobin-2 domain as an entity, to our knowledge, does not occur outside the vascular plants, we were wondering whether the isolated subdomains (A1, A2, A3, B1, and B2) might have additional homologues. For this purpose, we conducted a BLAST search with the isolated subdomains at reduced stringency of the *e*-value threshold (100) to recover such additional partial homologues whose functional assignments might give us an idea about potential cellular functions of ginkbilobin-2.

For the A1 motif, among 12 recovered hits, three of the homologues were part of the so-called CLASP-N-like/armadillo fold proteins. These cytoskeletal proteins are known to mediate interactions between actin filaments and microtubules. Two of those proteins were from insects, one from an oomycete with up to 65 % similarity that remained confined to the A1 motif. A search with the A2 motif yielded 13 hits, whereby six were two-component histidine kinases of plant-interacting bacteria. The homology was located at the start of the histidine-kinase homodimerization domain and reached up to 80 % similarity, again remaining confined to this motif on both sides. Whereas a search with the A3 motif did not uncover any homologues, the search with the B1 motif only produced a couple of angiosperm sequences (both mono- and dicots) in addition to the previously known ginkbilobin-2-containing proteins. These additional sequences also possess the above-mentioned specific cysteine signatures and showed homologies of 50–60 % similarity in most cases that were, however, confined to the B1 motif. For most of them no function was assigned. Three of these hits belonged to a plant receptor-like kinase superfamily involved in pathogen sensing (Chen 2001). A search with the B2 domain yielded not only homologues in bacterial proteins related to phytopathogenicity but also one plant DUF26 domain protein that had already been picked up by the search for B1 homologues. It should be noted that the hits recovered by this strategy shared only similarity with individual subdomains of ginkbilobin-2, not with ginkbilobin-2 as an entity. Nevertheless, these motifs indicate a putative relationship with defence on the one hand and with the cytoskeleton on the other.

Localization of full-length ginkbilobin-2 and its individual domains

To acquire more information about cellular functions of ginkbilobin-2, the subcellular localization of the full-length protein and specific truncations were investigated by expressing GFP fusions in tobacco BY-2 cells either transiently (by biolistics) or in a stable manner (using binary vectors based on the GATEWAY® cloning strategy). Since the N terminus harboured a predicted signal peptide of 26 amino acids (using the on line software SignalP 4.1 server), we first tested a fusion of GFP C-terminal to this putative signal motif. Upon expression, this construct showed up small fluorescent vesicles (Fig. 2a) that were moving along with the cytoplasmic strands and also decorated the nuclear rim, which indicated

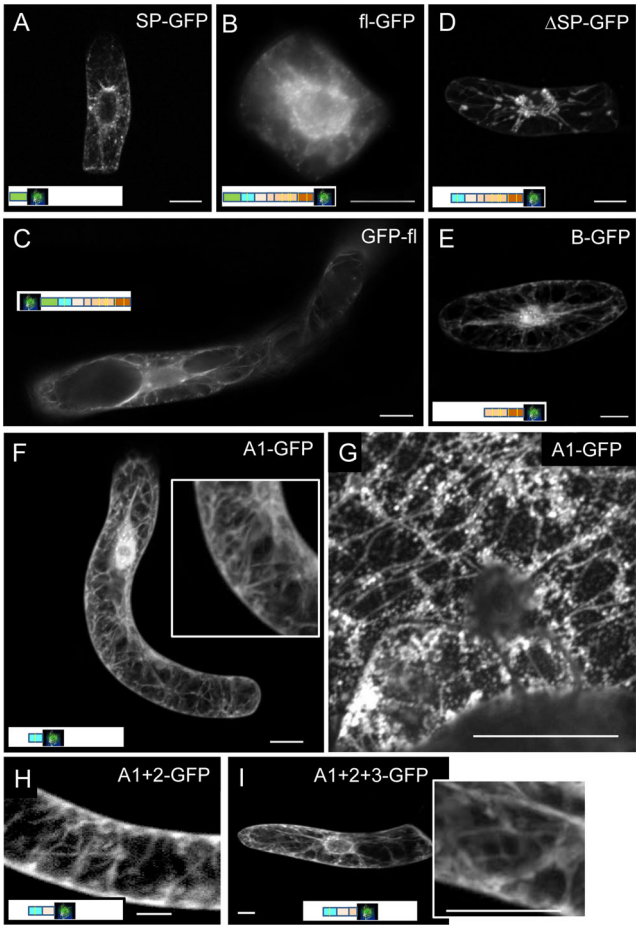

Fig. 2 Localization of GFP fusion constructs of full-length or truncated ginkbilobin-2 upon transient expression in tobacco BY-2 cells. The structure of the constructs used is shown schematically as *inset*. **a** Signal peptide upstream of GFP. **b** Full-length ginkbilobin-2 including the signal peptide upstream of C-terminally fused GFP. **c** Full-length ginkbilobin-2 including the signal peptide downstream of N-terminally fused GFP. **d** Ginkbilobin-2 lacking the signal peptide upstream of C-terminally fused GFP. **e** Subdomain B upstream of C-terminally fused GFP. **f** Subdomain A1 upstream of C-terminally fused GFP with a zoom-in to show the filaments visualised by this construct. **g** Confocal section of the cortical region for the same construct as in (**f**) to show punctate structures aligned as bead on a string along filaments. **h** Subdomains A1+A2 upstream of C-terminally fused GFP. **i** Subdomains A1+A2+A3 upstream of C-terminally fused GFP with a zoom-in to show the filaments visualised by this construct. *Scale bar* 20 μm

that the signal peptide was functional and designated GFP for secretion.

In the next step, the full-length ginkbilobin-2 (including the signal motif) was studied. Considering the presence of the signal peptide and potential steric hindrance, GFP was fused either in N- or in C-terminal position of the full-length ginkbilobin-2 coding sequence including the signal peptide. The C-terminal fusion of full-length ginkbilobin-2 (Fig. 2b) produced a similar pattern as the signal peptide alone, suggesting that the signal peptide was functional in committing its cargo for the secretory pathway. However, when GFP was fused to the N terminus of full-length ginkbilobin-2 (including the signal peptide), this fusion exhibited a different pattern (Fig. 2c) as it visualized filamentous structures that tethered the nucleus by transvacuolar strands to a cortical meshwork, a morphology and organization that is characteristic for plant actin. To test whether this deviant localization of GFP-ginkbilobin-2 was caused by GFP masking the signal peptide, we fused GFP C-terminally of full-length ginkbilobin-2, but truncated the signal motif (ΔSP). The pattern produced by this construct visualized wide strands that locally extended into lentil-shaped structures resembling the endoplasmic reticulum (Fig. 2d). Thus, ginkbilobin-2–if not sequestered from the cytoplasm by means of the N-terminal signal peptide–tethers to a filamentous network that might be actin.

We then asked which of the subdomains confer this specific localization. Thus, various subdomains or combinations thereof were tested for their localization. Subdomain B (Fig. 2e) that contains the specific cysteine signature was at first sight localized in a manner similar to the full-length protein with truncated signal peptide (Fig. 2d). However, a closer look reveals that the strands labelled by this construct are much broader and widen near the cell cortex into triangles, which is the pattern observed for the structure of the cytoplasmic strands in these vacuolated cells. This indicates that the filamentous localization of the full-length protein (Fig. 2c) is not conferred by domain B. Therefore, domain A was put under closer scrutiny: the entire domain A marked, in addition to cytoplasmic strands, slender and branched filaments (Fig. 2i, inset), which is characteristic for actin. Also, a combination of subdomains A1 and A2 produced filaments (Fig. 2h), and when everything was truncated down to subdomain A1 alone (Fig. 2f), a rich system of fine filaments became manifested that was congruent with the pattern observed for the full-length protein with truncated signal peptide. These filaments converged to the nuclear envelope and emanated from rod-like, sometimes more punctate structures at the nuclear rim. Confocal sections in the cortical region show that the punctate structures are aligned along filaments like beads on a string (Fig. 2g). This pattern is reminiscent of the actin cytoskeleton in those cells. This truncation study assigns the specific localization of ginkbilobin-2 to subdomain A1. It should be mentioned that for those constructs producing the actin-like patterns (i.e. full-length ginkbilobin without signal peptide, domain A, and its subdomains), the expressing cells had died a few days later.

Ginkbilobin-2 domains target to actin

To get insight into the cellular nature of the filamentous structures visualized by ginkbilobin-2, the different constructs described above were transiently expressed in a stable actin maker line expressing FABD2-RFP, either via biolistic or via agrobacteria-mediated transformation. When GFP was fused

to the N terminus of the full-length ginkbilobin-2 (Fig. 3a1–a3), filamentous structures were visualized that were congruent with actin filaments. In contrast, a fusion of GFP placed at the C-terminal of full-length ginkbilobin-2 (Fig. 3b1–b3) as well as the signal peptide alone (Fig. 3c1–c3) produced vesicles that were moving along the actin filaments. Next, we want to test whether the differential localization of N-terminal (Fig. 3a1–a3) versus C-terminal (Fig. 3b1–b3) GFP fused to full-length ginkbilobin-2 was caused by masking of the signal peptide, when GFP was fused at the N terminus. We thus generated a construct, where GFP was placed at the C terminus of full-length ginkbilobin-2 but where the signal peptide was truncated. This construct (ΔSP, Fig. 4a1–a3) visualized a subset of actin filaments. Exemplarily for the subdomains, we tested subdomain A1 (Fig. 4b1), which also colocalized with actin filaments. Also, when this subdomain was expressed in a wild-type background (Fig. 4b2), punctate structures like beads on a string labelled a fine meshwork subtending the plasma membrane in the same manner as cortical actin filaments.

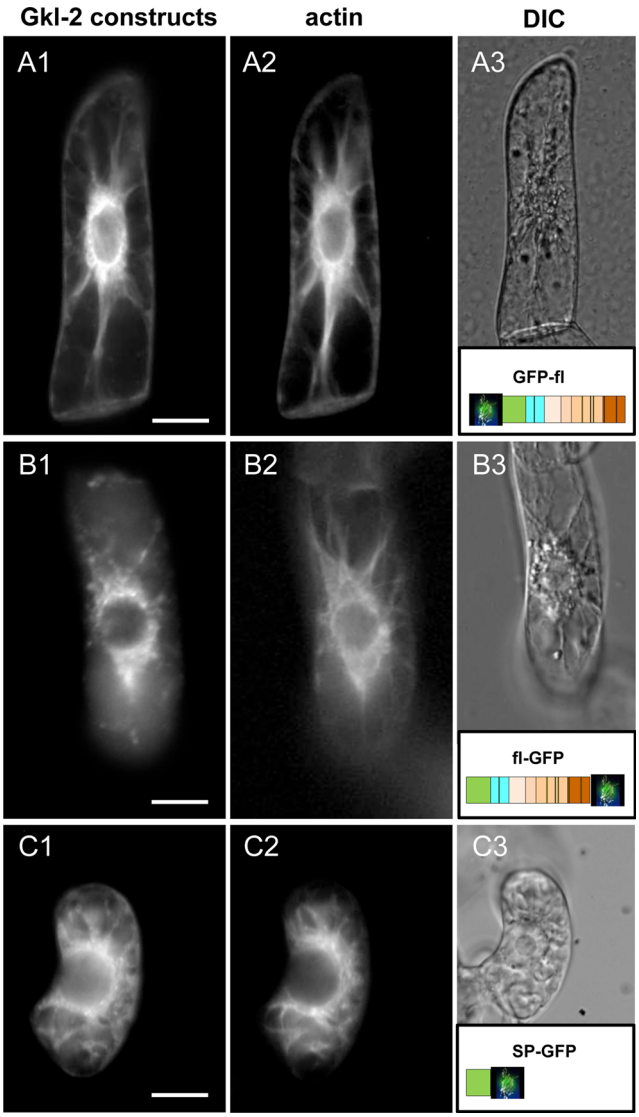

Fig. 3 Localization patterns observed for expression of ginkbilobin-2 fused with GFP in the background of the actin marker line RFP-FABD2. *1* showing the GFP signal, *2* the RFP signal, and *3* the dic channel. The *schematic sketch* shows the structure of the respective construct. **a** Full-length ginkbilobin-2 downstream of N-terminally fused GFP. **b** Full-length ginkbilobin-2 including the signal peptide upstream of C-terminally fused GFP. **c** Signal peptide upstream of C-terminally fused GFP. *Scale bar* 20 μm

To verify whether the localization of subdomain A1 was dependent on actin filaments, 1 μM of latrunculin B was used to treat cells expressing subdomain A1 for 30 min. Latrunculin B is commonly used to disrupt the actin cytoskeleton network (Spector et al. 1983), and indeed we find that the filamentous structures visualized by the GFP fusion with subdomain A1 (Fig. 2f, g) were completely eliminated and replaced by vesicular structures (Fig. 5a). The same was true for ginkbilobin-2 with GFP fused C-terminally but devoid of the signal peptide (Fig. 5b). As a control, the actin marker line GF11 was subjected to the same treatment and found to be devoid of any actin filaments, demonstrating that the treatment is efficient to eliminate actin microfilaments (Fig. 5c). A stable line of subdomain A1 in fusion with GFP showed the same filamentous structures as already seen in the transient transformants (compare Figs. 2 and 4). To verify if these filaments represent actin filaments, the stable transformants were stained with TRITC-phalloidin, a dye known to bind to polymeric actin (Kakimoto and Shibaoka 1987). The resulting images (Fig. 5d1–d3) showed that the GFP fusion of subdomain A1 (Fig. 5d1) colocalized with the TRITC-phalloidin labeled actin (Fig. 5d2).

The filamentous localization of ginkbilobin and its subdomains, their colocalization with TRITC-phalloidin labelled F-actin, and the loss of the filamentous localization after treatment with latrunculin B show that ginkbilobin-2—if not recruited for secretion by the signal peptide—binds to actin filaments, and that subdomain A1 is functionally equivalent to the full-length protein with respect to this actin-binding activity. However, whether subdomain A1 binds directly to actin or whether the interaction is mediated by third proteins cannot be decided from these in vivo data.

Subdomain A1 is necessary and sufficient to modulate nuclear positioning

To see whether the association of ginkbilobin-2 with actin would alter any actin-dependent cellular responses, different stable overexpression lines were generated in tobacco BY-2 via agrobacteria-mediated transformation and phenotyped. Stable transformants were obtained for subdomains A1, B, and full-length ginkbilobin-2 without the signal peptide (ΔSP, also abbreviated as NSP for 'non-signal peptide'). Subdomain A1 localized along transvacuolar actin cables and in rod-like punctate structures adjacent to the nuclear

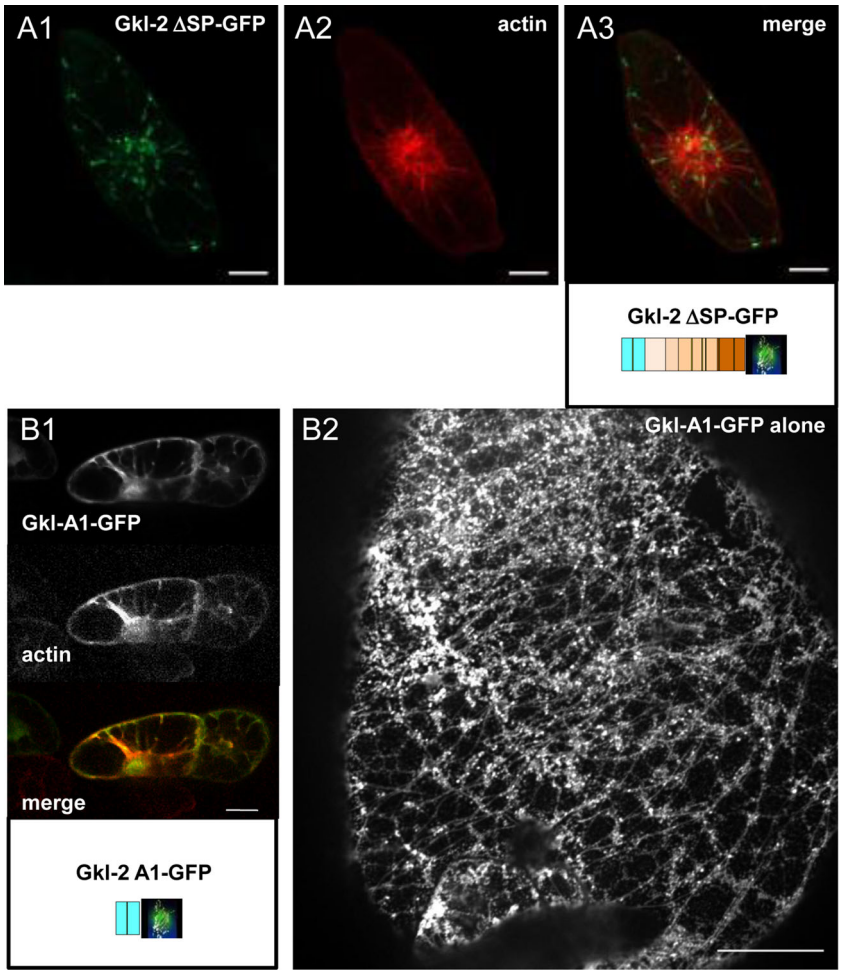

Fig. 4 Localization patterns observed for expression of ginkbilobin-2 subdomains fused with GFP in the background of the actin marker line RFP-FABD2 and BY-2 WT. **a** Ginkbilobin-2 lacking the signal peptide upstream of C-terminally fused GFP (NSP): *a1* showing the GFP signal, *a2* the RFP signal, and *a3* the merge of both signals. **b** Subdomain A1 upstream of C-terminally fused GFP: *b1* Subdomain A1 upstream of C-terminally fused GFP in the background of the actin marker line RFP-FABD2. *b2* The cortical layer of subdomain A1 of C-terminally fused GFP in a BY-2 WT background. The *schematic sketch* shows the structure of the respective construct. *Scale bar* 20 μm

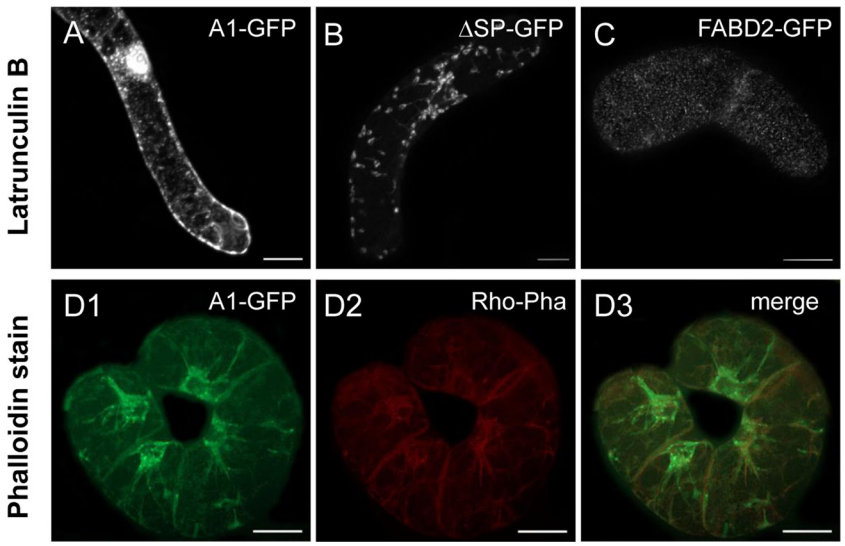

Fig. 5 The filamentous signal visualized by the subdomain A1 of ginkbilobin-2 is caused by actin. **a** Subdomain A1 upstream of C-terminally fused GFP after treatment with 1 μM of latrunculin B for 30 min. **b** Ginkbilobin-2 lacking the signal peptide upstream of C-terminally fused GFP (ΔSP) treated with 1 μM of latrunculin B for 30 min. **c** Actin signal in the GF-11 line after treatment with 1 μM of latrunculin B for 30 min. **d** Labelling of actin filaments in a stable transformant expressing subdomain A1 upstream of C-terminally fused GFP using TRITC-phalloidin. The GFP signal is shown in (*1*), the phalloidin signal in (*2*), the merge of both signals in (*3*). *Scale bar* 20 μm

rim (Figs. 5d1–d3, 6a). Generally, the signal in the stable transformants was weaker as compared to the transient expressors. Also, for the lines overexpressing NSP or subdomain B (Fig. 6b, c), only weak expression could be obtained that was localized in the same pattern as seen in the transiently transformed cells (Fig. 2e, d). This suggests that higher stable expression of the transgenes (especially prominent for NSP or subdomain B) might impair viability, such that during the course of cultivation only the weak expressors had persisted.

Premitotic nuclear positioning is a trait that depends on a perinuclear array of actin filaments (Durst et al. 2014) that move and tether the nucleus in concert with microtubules, plant-specific minus-directed KCH-kinesins, and the cortical meshwork of actin (Kühn et al. 2013). We therefore measured nuclear positioning on day 3 after subcultivation and observed that nuclear positioning was significantly delayed in the overexpressor of subdomain A1 (Fig. 6d) and NSP, compared to the non-transformed BY-2 control. In contrast, overexpression of subdomain B did not cause a significant delay. The comparison of the isolated subdomain A1 with the NSP construct (that also harbours subdomain A1 but did not produce a stronger effect) and with subdomain B demonstrates that subdomain A1 is necessary and sufficient to confer an inhibition on nuclear positioning. Nuclear migration is delayed by overexpression of a class-XIV kinesin, KCH (Frey et al. 2010), and this is followed by a corresponding delay of mitotic activity. To test whether also the delay of nuclear positioning by overexpression of subdomain A1 and the NSP construct would cause a delay of mitotic activity, we followed the time course of mitotic index for the transgenic lines (Suppl. Fig. 1) and found that the peak of mitotic activity was delayed by 1 day.

Actin-binding ginkbilobin-2 peptides conjugated to a cell-penetrating peptide induce programmed cell death

The attempt to generate stable overexpression cell line of the GFP fusions with ginkbilobin-2 fragments was only partially successful because the signal observed in the transformants was relatively low (see Fig. 6a–c) compared to the signal conferred by transient expression (see Fig. 2). This indicates that the overexpression of these transgenes impinges on viability, such that weaker expressors are favoured over stronger expressors. The stringency of antibiotic selection (100 $mg \cdot l^{-1}$ kanamycin) was already at the maximum–further increase of stringency would therefore cause sublethality even of transformed cells. We therefore employed a different strategy: The cell-penetrating peptide (CPP) BP100 can carry functional cargoes into plant cells (Eggenberger et al. 2011), which allows to administer a defined quantity of the function at any

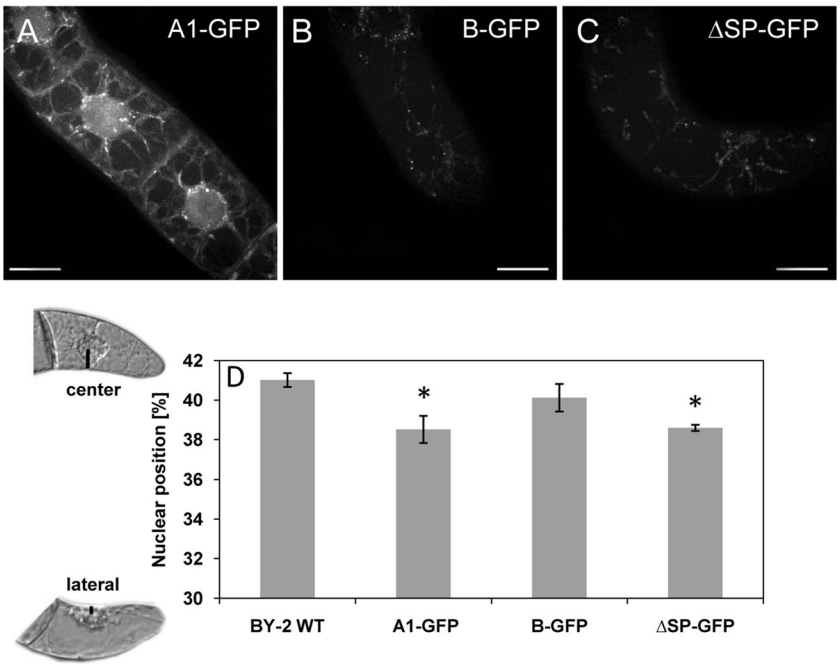

Fig. 6 Phenotypes of stable transformants and the nuclear positioning. Phenotypes of stable transformants for C-terminal GFP fusions with subdomain A1 (**a**), subdomain B (**b**), or the ΔSP construct, i.e. ginkbilobin without signal peptide (**c**). *Scale bar* 20 μm. Nuclear positioning in the stable transformants shown in (**a**–**c**) as compared to the non-transformed control (**d**). A value of 30 % indicates that the nucleus is completely lateral, whereas a value of 50 % indicates that the nucleus has moved exactly into the cell centre. Values represent means and standard errors from 1500 individual cells collected from three independent experimental series. *Asterisks* represent differences with the control that are significant at the 95 % confidence level

defined point in time. Therefore, various subdomains of ginkbilobin-2 were coupled with rhodamine B (RhB) as a fluorescent reporter and conjugated with BP100 by chemical synthesis and then introduced into BY-2 WT cells. Since the previous experiments had shown that the actin-binding activity can be mainly attributed to subdomain A, the conjugates were prepared for subdomains A1, A2, and A3, respectively. Our specific aim here was to identify which of the three subdomains are responsible for binding to actin.

Preparatory experiments demonstrated that treatment with the subdomain-CPP conjugates caused rapid cell death, if the concentration exceeded 1 μM. To follow uptake microscopically, we thus used 0.5 μM of the ginkbilobin-2 subdomain-CPP conjugates as well as the non-conjugated BP100 and incubated non-transformed BY-2 WT cells for 24 h to test the uptake by spinning-disc microscopy. Confocal sections near the central plane of the cell demonstrated clearly that the fluorescent marker was present in the cytoplasm (Fig. 7a–d). For the conjugates with subdomains A1, A2, and A3, the signal was forming punctate structures. Some of these dots seemed to be aligned like beads on a string (Fig. 7a–c, shown with arrows). RhB coupled with BP100 alone was also transferred into the cytoplasm but produced diffuse labelling throughout the cytoplasm and was also bound along the cross wall (Fig. 7d). To obtain more information about the localization of the peptides, the stable actin marker cell line GF-11 was incubated with the conjugates. The structures visualized by the subdomain A1 conjugate (Fig. 7e1) were associated with the transvacuolar actin cables. The fluorescence of the actin cables also appeared somewhat discontinuous. A similar outcome was observed for the subdomain A3 (Fig. 7g1–g3). In contrast, for subdomain A2 and the non-conjugated BP100 (Fig. 7f, h), the RhB signal did not colocalize with actin filaments, which also were of contiguous appearance. Here, also a considerable fraction of the RhB signal was associated with the cross walls. A quantification of apparent filament thickness *w* and filament density (Chang et al. 2015) showed that the A1 and A3 conjugates increased *w* almost threefold compared to a mock control, while reducing filament density by a similar factor, in contrast A2 was less effective (supplemental Table 5)

In the next step, we analysed the cell-death response triggered by the conjugates in more detail, by employing the uptake of the non-permeable dye Evan's Blue as readout for mortality. A dose-response of mortality, scored 1 h after addition of the conjugates, showed a threshold at 1 μM and saturation (with 100 % mortality) from 2 μM (Fig. 8a). As a control, we tested the non-conjugated BP100 carrier but observed only a minor induction of mortality (saturating at around 25 % from 2 μM), demonstrating that the high mortality is caused by the ginkbilobin peptide cargo and not by the carrier itself. Since the concentration range between threshold and saturation was very narrow if assessed at 1 h, potential

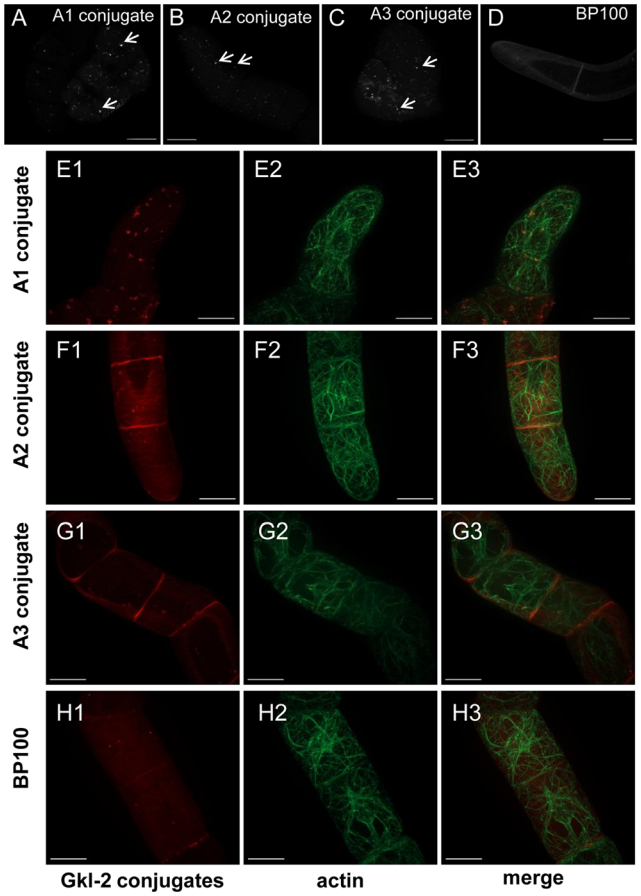

Fig. 7 Localization of ginkbilobin peptide conjugates in BY-2 cells. Introduction of ginkbilobin-2 peptide conjugates with the cell-penetrating peptide BP100 and rhodamine B as a fluorescent reporter into non-transformed cells of BY-2 (**a**–**d**), or into the actin marker line GF11 expressing the actin-binding domain 2 of plant fimbrin in fusion with GFP (**e**–**h**). **a**, **e** Subdomain A1. **b** **f** Subdomain A2. **c**, **g** Subdomain A3. **d**, **h** Non-conjugated BP100. Panels (*1e–1h*) show the rhodamine signal, (*2*) the actin signal, and (*3*) the merge of both signals, respectively. Incubation time 1 h. *Arrows* show the punctate structures. *Scale bar* 20 μm

differences between the peptides were hardly resolved. We therefore followed the time course of mortality for a concentration of 1 μM (Fig. 8b). Here, mortality developed most rapidly for the A1 and A3 conjugates, whereas A2 produced a weaker effect. As negative control, the carrier, BP100, was used alone, without any fused ginkbilobin conjugate. In the absence of ginkbilobin, BP100 did not cause significant mortality, even after incubation for 24 h (Fig. 8b). Thus, those conjugates that decorated actin cables (A1 and A3) were also effective in inducing cell death, whereas the A2 conjugate that did not decorate actin cables was also a less efficient trigger of cell death.

To probe the role of actin in this cell-death response, we pretreated the cells prior to addition of the conjugates for 30 min with compounds acting directly or indirectly upon actin: 1 μM latrunculin B, sequestering G-actin from

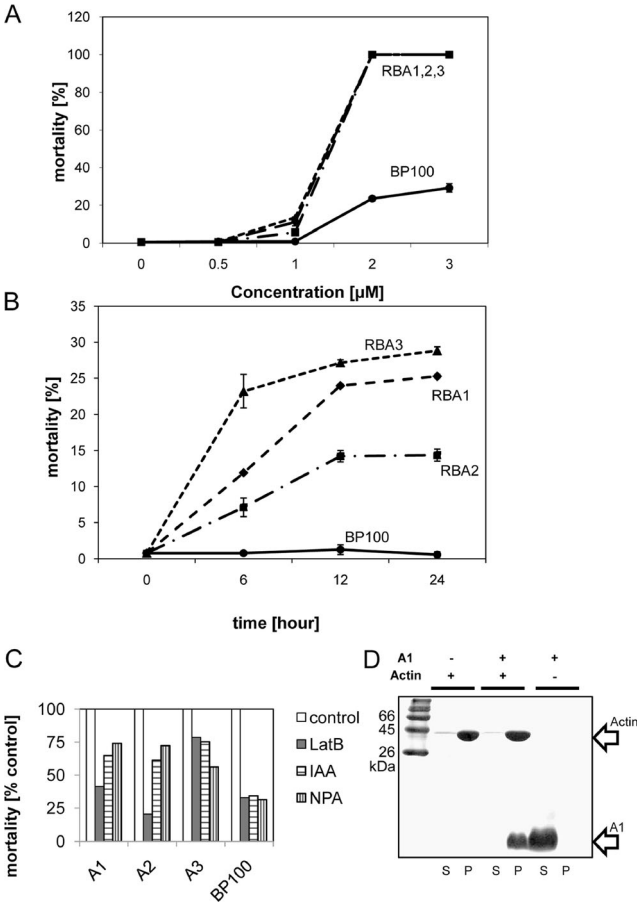

Fig. 8 Activity of ginkbilobin peptide conjugates in vivo and in vitro. Induction of cell death in vivo (**a**–**c**) and binding to actin in vitro (**d**). Dose-response (**a**) and time course (**b**) of mortality after treatment with rhodamine-labelled conjugates of BP100 with subdomains A1 (RBA1, *diamonds*), A2 (RBA2, *squares*), or A3 (RBA3, *triangles*) respectively versus BP100 alone (RBP100, *circles*). Dose-response (**a**) measured after treatment for 1 h, time course (**b**) measured for treatment with 1 μM of the same conjugates as in (**a**). Mortality observed 6 h after addition of the conjugates after pretreatment for 30 min with either latrunculin B (1 μM), the natural auxin IAA (2 μM), or the auxin-efflux inhibitor NPA (10 μM), respectively (**c**). Values are represented relative to the control (treatment with the respective conjugate, but without pretreatment). Data represent mean values and standard errors from three independent experimental series comprising a population of more than 3000 cells for each curve. Coassembly of ginkbilobin A1 conjugates with BP100 with actin in vitro (**d**). F-actin was assembled for 1 h at 22 °C either in the presence or absence of A1-conjugate and then precipitated by ultracentrifugation. As negative control, A1-conjugate was incubated in parallel without G-actin. Supernatant (*S*) and precipitate (*P*) were separated side by side by SDS-PAGE and stained by Coomassie Brilliant Blue

integration into filaments, and 2 μM of exogenous natural auxin, causing dissociation of actin cables into finer strands or complete inhibition of auxin efflux by 10 μM of the auxin-efflux blocker 1-naphthyl phthalamic acid (NPA). The concentrations and effects of these compounds had been characterized for the same cell line in a previous publication (Durst et al. 2013). We observed that all these treatments strongly reduced the mortality (scored 6 h after addition of the conjugates) induced by 1 μM of the conjugates (Fig. 8c), indicating that actin dynamics is necessary for conjugate-triggered cell death. To test whether this response meets criteria of programmed cell death, we labelled cells treated for 3 h with the A1-conjugate (again 1 μM) with TdT-mediated dUTP-biotin nick end labeling (TUNEL) and DAPI. We observe that many of the A1-treated cells showed TUNEL-positive nuclei (supplemental Fig. 2A), whereas in the controls the TUNEL signal was not significant. At 6 h, many of the A1-treated nuclei showed clear symptoms of disintegration (supplemental Fig. 2B). When the frequency of TUNEL-positive nuclei was scored (supplemental table 4), it was found to be almost 50 % for the A1-conjugate, even higher for the A3-conjugate, but only around 30 % for the A2-conjugates. In contrast, BP100 alone or a non-treated mock control produced only some 10 % TUNEL-positive nuclei.

We further assayed for a potential antifungal activity of the conjugates (supplemental Table 3) using *C. albicans* as experimental model. We observed that rhodamine-labelled conjugates of BP100 with subdomains A1, A2, and A3 reached the same inhibition as the positive control gramicidin S, whereas there was no significant inhibition (as for rhodamine alone or 50 % ethanol used as negative controls) when rhodamine was directly linked to the subdomains and BP100 was omitted.

To test whether the ginkbilobin subdomain A1 can bind to actin directly, we performed a coassembly assay (Fig. 8d): G-actin was assembled into F-actin either in the absence or presence of A1 conjugate, and the filaments were then collected by ultracentrifugation. In the presence of G-actin, the A1 conjugate was quantitatively partitioned to the precipitate along with actin itself. A negative control, where the A1 conjugate was incubated in parallel in absence of G-actin left the A1 conjugate in the supernatant, verifying that the actin-dependent precipitation was specific and not caused by unspecific agglomeration of the peptide conjugate.

Discussion

Potential functions of ginkbilobin domains

The binding of ginkbilobin to actin was shown to be mediated by the subdomain A1 (Figs. 2 and 4), and it was necessary and sufficient for the delay of premitotic nuclear positioning (Fig. 6). In contrast, subdomain A2 appeared to be dispensable for actin binding. The tertiary structure of ginkbilobin-2 has been solved based on crystallization and is composed of two α-helices and a β-sheet composed of five strands, which form a compact single-domain architecture comprising the α-helices and the β-strands (Miyakawa et al. 2009). One of the α-helices produced by subdomain A2 constitutes a positively charged surface. This positively charged surface of subdomain

A2 was suggested to interact with the (negatively charged) fungal surface, which might cause membrane permeabilization analogous to the case of sapecin, an insect defensin (Takeuchi et al. 2004). Subdomain B contains a specific and conserved cysteine signature (C-X_8-C-X_2-C) that is also characteristic of so-called DUF-26 homologues, a subgroup of the extensive receptor-like kinase superfamily of angiosperms. This subgroup of cysteine-rich receptor-like kinases is involved in plant defence to pathogen attack (Czernic et al. 1999). The conserved cysteine signature forms three disulfide bridges that are likely to contribute to the structural stability of ginkbilobin (Miyakawa et al. 2009) and by functional analogy might act in pathogen recognition. The functional context of this putative pathogen recognition is certainly different: in *G. biloba*, the B-domain would target the actin-binding subdomain A1 to the pathogen, whereas in the context of the cysteine-rich receptor-like kinases of angiosperms, the recognition of the pathogen would trigger an intracellular kinase cascade culminating in the activation of defence genes and, in the case of a biotrophic pathogen, programmed cell death.

Advances in chemical engineering using functional cargoes

We have shown in previous work (Eggenberger et al. 2011) that BP100 can be used as an efficient cell-penetrating carrier to enter living plant cells. This tool can be exploited for chemical engineering, by conjugating specific peptides that bind to specific cellular targets as cargo to BP100. As a proof of principle, the actin-binding peptide Lifeact had been successfully introduced into tobacco cells using BP100 and used to visualize the perinuclear actin network. Those earlier experiments by Eggenberger et al. (2011) have shown that Lifeact coupled to BP100 can be introduced into BY-2 cells and binds to the actin microfilaments, while Lifeact without BP100 can also be taken up by the cells but the Lifeact has no function that only localizes in the cytoplasm. Cell-penetrating peptides (CPPs) are short cationic peptides with an amphiphilic character that interact with the negatively charged cell surface and can finally pass through the hydrophobic lipid bilayer without causing any permanent damage. Although short cationic sequences with an amphiphilic nature seem to be required in CPPs to enable their membrane passage, the mechanism of this bilayer penetration is still unclear (Fischer et al. 2004; Pujals et al. 2006; Fonseca et al. 2009). However, irrespective of the still enigmatic mechanism of uptake, the current work demonstrates that CPPs can be successfully used to introduce functional cargoes (in this case subdomain A1 of ginkbilobin) into living plant cells to obtain a specific cellular response namely programmed cell death, while ginkbilobin subdomains without BP100 have no cellular effect.

Actin as a deadly switch

Premitotic nuclear positioning depends on a perinuclear cage of actin filaments and microtubules that are linked by KCH kinesins (Kühn et al. 2013). The development of mitotic activity of subdomain A1 overexpressor matches the observations for the nuclear movement consistent with published work showing that the nuclear positioning acts as pacemaker for the first division (Fig. 6d and supplemental Fig. 1).

Our observations indicate a role of actin reorganization for the induction of programmed cell death. It should be emphasized that the ginkbilobin conjugates do not eliminate actin filaments but rather seem to induce a network of more massive actin cables (Fig. 2c). This impression is also supported by quantifications of apparent filament thickness and filament density in response to treatment with the subdomain A conjugates (supplemental table 5): Here, a reduction of filament density is accompanied by a corresponding increase in apparent filament thickness indicative of a bundling process. Also the in vitro coassembly data (Fig. 8d) speak against an eliminating activity of ginkbilobin. Low concentrations of latrunculin B sequester free G-actin that otherwise would be recruited for polymerization and thus impair the formation of bundles. Exogenous natural auxin prevents bundling through a different mechanism, by releasing actin-depolymerization factors from their membrane anchor PIP2 (Durst et al. 2013), and the phytotropin NPA blocks auxin efflux, thus causing elevated levels of auxin. All three treatments can significantly reduce ginkbilobin-induced cell death leading to the conclusion that actin dynamics is necessary to trigger cell death in response to the ginkbilobin conjugates (Fig. 8c). The link between actin and auxin is further corroborated by the finding that auxin can mitigate Harpin-induced actin bundling and cell death in grapevine cells by competition for superoxide generated by the membrane-located NADPH oxidase (Chang et al. 2015).

Although actin bundling is reduced by auxin, the effect of auxin on cell death is no direct proof for a role of bundling because auxin might also act through a parallel pathway. To test the role of actin bundling for ginkbilobin activity directly, we therefore plan experiments with a cell line expressing the actin bundling WLIM domain under control of an inducible promoter. In this cell line, upon induction of the promoter by dexamethasone, the expression of WLIM causes progressive actin bundling (Hohenberger et al. 2011). The observation of TUNEL-positive nuclei and disintegrating nuclei support the conclusion that the ginkbilobin-induced response meets criteria for programmed cell death. The interaction of ginkbilobin with actin might be direct or indirect through actin-binding proteins. We therefore tested for the A1 conjugate, whether it can bind to actin in vitro, and found that A1 can specifically coassemble with G-actin into filaments indicative of direct interaction with actin. Actin-dependent

programmed cell death is a topic progressively emerging for eukaryotic cells in general (for reviews see Gourlay and Ayscough 2005; Franklin-Tong and Gourlay 2008). Despite the molecular differences between programmed cell death in plants and classical apoptosis, the dependence on actin has also been demonstrated for plant cells (reviewed in Smertenko and Franklin-Tong 2011) and seems to represent an evolutionarily conserved aspect of programmed cell death. For instance, the bundling of actin cables in cells of the embryonic suspensor not only heralds ensuing cell death but has been shown to be necessary and sufficient to initiate this response (for review see Smertenko and Bozhkov 2014). We also could demonstrate in suspension cells of grapevine and tobacco that cell death triggered by bacterial Harpin elicitors is heralded by a rapid and specific reorganization of the actin cytoskeleton: The cortical actin filaments subtending the cell membrane detach, and the entire actin skeleton contracts into dense cables towards the nucleus (Qiao et al. 2010, response of *Vitis rupestris* to Harpin N; Guan et al. 2013, response of tobacco BY-2 to Harpin Z). Moreover, the grapevine phytoalexin resveratrol, which seems to be crucial for resistance to biotrophic pathogens, can induce a similar actin response, which is later followed by programmed cell death (Chang et al. 2011).

Based on the functional study conducted in the present work, a working model for the biological function of ginkbilobin can be proposed: Interference of subdomain A with the actin of the producer cell is prevented by efficient secretion of the protein by virtue of its N-terminal signal peptide. Upon secretion, ginkbilobin could reach microbial surfaces, where the actual 'killer', i.e. subdomain A would take effect. The activity of subdomain A seems to be located mainly in subdomains A1 and A3. The polar growth of fungal hyphae depends on the actin cytoskeleton (Pruyne and Bretscher 2000a, b) sustaining very intensive recycling of membraneous material at the hyphal tip including numerous membrane fusion and separation events (Ayscough et al. 1997). These events are highly dependent on actin turnover and therefore represent a very sensitive target for compounds with antifungal activity. When ginkbilobin binds to the hyphal tip, it is expected to enter the cell as a consequence of intensive membrane recycling events and will eventually come into contact with actin filaments to bind and interfere with their dynamicity. The fact that conjugates of the A1-A3 peptides with BP100 block growth of *C. albicans* more efficiently than conjugates of A1-A3 with rhodamine might indicate that entrance into the target cell is limiting for the efficacy (although it should be kept in mind that the direct conjugation with rhodamine might also sterically impede the effect of the peptide). As a consequence, polar growth is arrested. Moreover, suppression of actin dynamicity can induce apoptotic cell death also in fungi, a phenomenon known in the literature as 'actin-mediated apoptosis' (Gourlay et al. 2004; Gourlay and Ayscough 2005, 2006). The antifungal activity of ginkbilobin has been demonstrated by plate inhibition assays (Wang and Ng 2000; Sawano et al. 2007) for different fungi such as *Fusarium oxysporum*, *Trichoderma reesei*, or *C. albicans*. Unfortunately, the cellular mechanism of growth inhibition has not been addressed in those studies.

Based on this working model, the antifungal activity of ginkbilobin would exploit an evolutionarily conserved and ancient mechanism to control cell death via restricting actin dynamics. Later, by a functional shift in higher plants, the functional modules of ginkbilobin seemed to have been recruited for different purposes; the cysteine signature of the B-domain was integrated into receptor-like kinases such that microbial binding could be linked with defence signalling. Therefore, the A-domain became dispensable and was lost in most proteins except for some protective proteins of the seeds (the homologues harbouring the long C-terminal extension). Future work will be dedicated to analyse the cellular response of fungal hyphae to ginkbilobin and its functional subdomains.

Acknowledgments This project was supported by the DFG-Center of Functional Nanostructure (CFN, projects E1.2 and E1.5) and a fellowship of the Chinese Scholarship Council to Ningning Gao. Technical support from Sabine Purper in the cultivation of the cell lines is gratefully acknowledged.

Conflict of interest We declare that we have no conflicts of interest to our work.

References

Ayscough KR, Stryker J, Pokala N, Sanders M, Crews P, Drubin DG (1997) High rates of actin filament turnover in budding yeast and roles for actin in establishment and maintenance of cell polarity revealed using the actin inhibitor latrunculin-A. J Cell Biol 137: 399–416

Banerjee RD, Sen P (1980) Antibiotic activity of pteridophytes. Econ Botany 34:284–298

Buschmann H, Green P, Sambade A, Doonan JH, Lloyd CW (2011) Cytoskeletal dynamics in interphase, mitosis and cytokinesis analysed through *Agrobacterium*-mediated transient transformation of tobacco BY-2 cells. New Phytol 190:258–267

Chang X, Heene E, Qiao F, Nick P (2011) The phytoalexin resveratrol regulates the initiation of hypersensitive cell death in Vitis cell. PLoS One 6, e26405

Chang X, Riemann M, Nick P (2015) Actin as deathly switch? How auxin can suppress cell-death related defence. PloS One. doi:10.1371/journal. pone. 0125498

Chen Z (2001) A superfamily of proteins with novel cysteine-rich repeats. Plant Physiol 126:473–476

Czernic P, Visser B, Sun W, Savoure A, Deslandes L, Marco Y, Van Montagu M, Verbruggen N (1999) Characterization of an *Arabidopsis thaliana* receptor-like protein kinase gene activated by oxidative stress and pathogen attack. Plant J 18:321–327

Diamond BJ, Shiflett SC, Feiwel N, Matheis RJ, Noskin O, Richards JA, Schoenberger NE (2000) *Ginkgo biloba* extract: mechanisms and clinical indications. Arch Phys Med Rehabil 81:668–678

Durst S, Nick P, Maisch J (2013) Actin-depolymerizing factor 2 is involved in auxin dependent patterning. J Plant Physiol 170:1057–1066

Durst S, Hedde PN, Brochhausen L, Nick P, Nienhaus GU, Maisch J (2014) Organization of perinuclear actin in live tobacco cells observed by PALM with optical sectioning. J Plant Physiol 171:97–108

Eggenberger K, Mink C, Wadhwani P, Ulrich AS, Nick P (2011) Using the peptide BP100 as a cell-penetrating tool for the chemical engineering of actin filaments within living plant cells. Chembiochem 12:132–137

Fields GB, Noble RL (1990) Solid phase peptide synthesis utilizing 9-fluorenylmethoxycarbonyl amino acids. Int J Pept Protein Res 35: 161–214

Finer JJ, Vain P, Jones MW, McMullen MD (1992) Development of the particle inflow gun for DNA delivery to plant cells. Plant Cell Rep 11:323–328

Fischer R, Kohler K, Fotin-Mleczek M, Brock R (2004) A stepwise dissection of the intracellular fate of cationic cell-penetrating peptides. J Biol Chem 279:12625–12635

Fonseca SB, Pereira MP, Kelley SO (2009) Recent advances in the use of cell-penetrating peptides for medical and biological applications. Adv Drug Deliv Rev 61:953–964

Franklin-Tong VE, Gourlay CW (2008) A role for actin in regulating apoptosis/programmed cell death: evidence spanning yeast, plants and animals. Biochem J 413:389–404

Frey N, Klotz J, Nick P (2010) A kinesin with calponin-homology domain is involved in premitotic nuclear migration. J Exp Bot 61: 3423–3437

Gourlay CW, Ayscough KR (2005) Identification of an upstream regulatory pathway controlling actin-mediated apoptosis in yeast. J Cell Sci 118:2119–2132

Gourlay CW, Ayscough KR (2006) Actin-induced hyperactivation of the Ras signaling pathway leads to apoptosis in *Saccharomyces cerevisiae*. Mol Cell Biol 26:6487–6501

Gourlay CW, Carpp LN, Timpson P, Winder SJ, Ayscough KR (2004) A role for the actin cytoskeleton in cell death and aging in yeast. J Cell Biol 164:803–809

Guan X, Buchholz G, Nick P (2013) The cytoskeleton is disrupted by the bacterial effector HrpZ, but not by the bacterial PAMP flg22, in tobacco BY-2 cells. J Exp Bot 64:1805–1816

Hohenberger P, Eing C, Straessner R, Durst S, Frey W, Nick P (2011) Plant actin controls membrane permeability. BBA Membr 1808: 2304–2312

Huang X, Xie W, Gong Z (2000) Characteristics and antifungal activity of a chitin binding protein from *Ginkgo biloba*. FEBS Lett 478:123–126

Jones JD, Dangl JL (2006) The plant immune system. Nature 444:323–329

Kakimoto T, Shibaoka H (1987) Actin filaments and microtubules in the preprophase band and phragmoplast of tobacco cells. Protoplasma 140:151–156

Karimi M, Inze D, Depicker A (2002) GATEWAY vectors for *Agrobacterium*-mediated plant transformation. Trends Plant Sci 7: 193–195

Kleijnen J, Knipschild P (1992) Ginkgo biloba. Lancet 340:1136–1139

Klotz J, Nick P (2012) A novel actin-microtubule cross-linking kinesin, NtKCH, functions in cell expansion and division. New Phytol 193: 576–589

Kubanek J, Jensen PR, Keifer PA, Sullards MC, Collins DO, Fenical W (2003) Seaweed resistance to microbial attack: a targeted chemical defense against marine fungi. Proc Natl Acad Sci U S A 100:6916–6921

Kühn S, Liu Q, Eing C, Frey W, Nick P (2013) Nanosecond electric pulses affect a plant-specific kinesin at the plasma membrane. J Membr Biol 246:927–938

Lin LC, Kuo YC, Chou CJ (2000) Cytotoxic biflavonoids from *Selaginella delicatula*. J Nat Prod 63:627–630

Liu J, Y.H. W, Q. W, Z.Z. L, A.G. G (2010) Purification and gene cloning of an antimicrobial protein from seeds of *Ginkgo biloba* L. J. Agric. Biotech. 18: 246–253

Maisch J, Nick P (2007) Actin is involved in auxin-dependent patterning. Plant Physiol 143:1695–1704

Maisch J, Fiserova J, Fischer L, Nick P (2009) Tobacco Arp3 is localized to actin-nucleating sites in vivo. J Exp Bot 60:603–614

Miyakawa T, Miyazono K, Sawano Y, Hatano K, Tanokura M (2009) Crystal structure of ginkbilobin-2 with homology to the extracellular domain of plant cysteine-rich receptor-like kinases. Proteins 77: 247–251

Nagata T, Nemoto Y, Hasezawa S (1992) Tobacco BY-2 cell line as the "Hela" cell in the cell biology of higher plants. Int Rev Cytol 132:1–30

Olyslaegers G, Verbelen JP (1998) Improved staining of F-actin and colocalization of mitochondria in plant cells. J Microsc 192:73–77

Parihar P, Parihar L, Bohra A (2010) In vitro antibacterial activity of fronds (leaves) of some important pteridophytes. J Microbiol Anti Microb 2:19–22

Ponce de Leon I, Montesano M (2013) Activation of defense mechanisms against pathogens in mosses and flowering plants. Int J Mol Sci 14: 3178

Pruyne D, Bretscher A (2000a) Polarization of cell growth in yeast. J Cell Sci 113(Pt 4):571–585

Pruyne D, Bretscher A (2000b) Polarization of cell growth in yeast. I. Establishment and maintenance of polarity states. J Cell Sci 113(Pt 3):365–375

Pujals S, Fernandez-Carneado J, Lopez-Iglesias C, Kogan MJ, Giralt E (2006) Mechanistic aspects of CPP-mediated intracellular drug delivery: relevance of CPP self-assembly. Biochim Biophys Acta 1758:264–279

Qiao F, Chang XL, Nick P (2010) The cytoskeleton enhances gene expression in the response to the Harpin elicitor in grapevine. J Exp Bot 61:4021–4031

Sano T, Higaki T, Oda Y, Hayashi T, Hasezawa S (2005) Appearance of actin microfilament 'twin peaks' in mitosis and their function in cell plate formation, as visualized in tobacco BY-2 cells expressing GFP-fimbrin. Plant J 44:595–605

Sawano Y, Miyakawa T, Yamazaki H, Tanokura M, Hatano K (2007) Purification, characterization, and molecular gene cloning of an antifungal protein from *Ginkgo biloba* seeds. Biol Chem 388:273–280

Severin FF, Hyman AA (2002) Pheromone induces programmed cell death in *S. cerevisiae*. Curr Biol 12:233–235

Shen G, Pang Y, Wu W, Deng Z, Liu X, Lin J, Zhao L, Sun X, Tang K (2005) Molecular cloning, characterization and expression of a novel Asr gene from *Ginkgo biloba*. Plant Physiol Biochem 43:836–843

Smertenko A, Bozhkov P (2014) The life and death signalling underlying cell fate determination during somatic embryogenesis. Appl Plant Cell Biol 22:131–178

Smertenko A, Franklin-Tong VE (2011) Organisation and regulation of the cytoskeleton in plant programmed cell death. Cell Death Differ 18:1263–1270

Spector I, Shochet NR, Kashman Y, Groweiss A (1983) Latrunculins: novel marine toxins that disrupt microfilament organization in cultured cells. Science 219:493–495

Srivastava J, Barber D (2008) Actin co-sedimentation assay; for the analysis of protein binding to F-actin. J Vis Exp 13:1–2

Takeuchi K, Takahashi H, Sugai M, Iwai H, Kohno T, Sekimizu K, Natori S, Shimada I (2004) Channel-forming membrane permeabilization by an antibacterial protein, sapecin: determination of membrane-buried and oligomerization surfaces by NMR. J Biol Chem 279: 4981–4987

Tsai PW, Yang CY, Chang HT, Lan CY (2011) Human antimicrobial peptide LL-37 inhibits adhesion of Candida albicans by interacting with yeast cell-wall carbohydrates. PLoS One 6, e0017755

van der Geer P, Hunter T, Lindberg RA (1994) Receptor protein-tyrosine kinases and their signal transduction pathways. Annu Rev Cell Biol 10:251–337

Wadhwani P, Afonin S, Ieronimo M, Buerck J, Ulrich AS (2006) Optimized protocol for synthesis of cyclic gramicidin S: starting amino acid is key to high yield. J Org Chem 71:55–61

Wadhwani P, Burck J, Strandberg E, Mink C, Afonin S, Ulrich AS (2008) Using a sterically restrictive amino acid as a 19F NMR label to monitor and to control peptide aggregation in membranes. J Am Chem Soc 130:16515–16517

Wang H, Ng TB (2000) Ginkbilobin, a novel antifungal protein from *Ginkgo biloba* seeds with sequence similarity to embryo-abundant protein. Biochem Biophys Res Commun 279:407–411

Weinberger F (2007) Pathogen-induced defense and innate immunity in macroalgae. Biol Bull 213:290–302

Wiegand I, Hilpert K, Hancock REW (2008) Agar and broth dilution methods to determine the minimal inhibitory concentration (MIC) of antimicrobial substances. Nat Protoc 3:163–175